Наносистеми, наноматеріали, нанотехнології
Nanosistemi, Nanomateriali, Nanotehnologii
2023, т. 21, № 2, сс. 413–426

PACS numbers: 68.37.Hk, 68.37.Vj, 81.07.Wx, 81.16.Be, 81.20.Ka, 81.70.Pg, 82.60.Hc

The Control of the Structure and Size of the Barium Titanate Nanoparticles Prepared by the Oxalate Method

O. A. Kovalenko[1,2], O. V. Shyrokov[1], V. G. Kolesnichenko[1,2], and A. V. Ragulya[1,2]

[1]*I. M. Frantsevych Institute for Problems of Materials Science, N.A.S. of Ukraine, 3, Omeljan Pritsak Str., UA-03142 Kyiv, Ukraine*
[2]*LLC 'NanoTechCenter', 3, Omeljan Pritsak Str., 3, UA-03142 Kyiv, Ukraine*

In this paper, the effect of the precipitation conditions and phase composition of the precursor on the mechanism of decomposition of intermediate compounds and the characteristics of the final product is shown. The stoichiometric barium titanate can be obtained from pure oxalate under concentration of 1.5 M and pH = 1. When composition is deviated from the stoichiometry, the final temperature of organic-precursor decomposition is increased above 720°C due to the multiphase-system formation. The crystallites formed during the thermal decomposition of precursors based on a multiphase system have smaller sizes (< 26 nm) compared to the decomposition product of pure oxalate (32–34 nm) due to the hydroxide and carbonate formation. At a concentration of 1.5 M, the decomposition of barium titanyl oxalate occurs due to the formation of intermediate oxycarbonates, rather than due to the oxidation of the precursor to barium carbonate and titanium dioxide. Applying nonisothermal mode for the calcination of the stoichiometric barium titanate allows the domination of the nucleation over the crystal growth resulting in the formation of monodisperse barium titanate with the crystallite and particle sizes of 22 nm and 25 nm, respectively. We suggest that the obtained results can be useful for the facile preparation of nanocrystalline stoichiometric barium titanate particles with desirable composition and size.

У даній роботі показано вплив умов осадження та фазового складу прекурсора на механізм розкладання проміжних сполук і характеристики кінцевого продукту. Стехіометричний титанат Барію можна одержати з чистого оксалату за концентрації у 1.5 М і pH 1. За відхилу складу від стехіометрії кінцева температура розкладання органічного прекурсора зростає вище 720°C завдяки утворенню багатофазної системи. Криста-

літи, що утворюються під час термічного розкладання прекурсорів на основі багатофазної системи, мають менші розміри (< 26 нм) порівняно з продуктом розкладання чистого оксалату (32–34 нм) за рахунок утворення гідроксиду та карбонату. За концентрації у 1.5 М розкладання титанілоксалату Барію відбувається за рахунок утворення проміжних оксикарбонатів, а не за рахунок окиснення попередника до карбонату Барію та діоксиду Титану. Застосування неізотермічного режиму випалу стехіометричного титанату Барію уможливлює досягти домінування зародкоутворення над ростом кристалу, що дає змогу одержати монодисперсний титанат Барію з розміром кристаліту та частинок у 22 нм та 25 нм відповідно. Ми припускаємо, що одержані результати можуть бути корисними для простого одержання нанокристалічних стехіометричних частинок титанату Барію бажаного складу та розміру.

Key words: barium titanate, stoichiometry, precipitation, nanoparticle, thermal decomposition, crystallization.

Ключові слова: титанат барію, стехіометрія, осадження, наночастинка, термічний розклад, кристалізація.

(Received 26 September, 2022; in revised form, 30 September, 2022)

1. INTRODUCTION

Barium titanate ($BaTiO_3$) has unique ferroelectric and dielectric properties and is widely used in capacitors [1]. The application of nanoscale $BaTiO_3$ particles makes it possible to obtain high-density ceramics and, therefore, improves the product properties. Moreover, reducing the particle size of $BaTiO_3$ in the polymer composite permits an increase in the permittivity value [1]. Also, to obtain a thin ceramic $BaTiO_3$ dielectric layer, high stoichiometry (Ba/Ti ratio in the range of 0.99–1.01), crystallinity, and dispersion characteristics in the suspension are required [2]. Thus, the control of the stoichiometry, size, and structure of the nanoparticle, which forms the ceramic material, presents a special field for the research. Such regulation of the particle characteristic may be realized through the selection of the appropriate synthesis method as well as thorough tuning of the synthesis parameters.

Among the existing methods of the preparation of $BaTiO_3$ nanoparticles as the high-temperature solid-state [3], sol–gel [4–6], hydrothermal [7, 8] ones, the most convenient chemical method in terms of the high-yield and low-cost production of stoichiometric nanopowder with a narrow size distribution, minimization of secondary phases, the ability to obtain a wide diversity of nanopowders under standard conditions, is the oxalate method (or Pechini method) [9–12], which include the step of deposition of the

organic metal-based complex from colloidal solutions, and the subsequent step of thermal decomposition of the obtained precursor to the final product.

The main characteristics of the precipitated barium titanyl oxalate are stoichiometry (Ba/Ti = 1), which allows the minimization of the secondary phases and obtaining the pure barium titanate. Another demand is the amorphous nature of the precursor, which facilitates the solid-phase diffusion in the next step of compound thermolysis and allows the adjustment of the final particle size. However, little attention is paid to the phase composition of the precipitated complex, its effect on the thermal decomposition of this compound, and the characteristics of the final product.

The literature data regarding the effect of the pH of the reaction medium on the phase of the precipitated precursor are contradictory (Fig. 1). Despite the possibility of the complete precipitation of metals with the pure perovskite formation at pH above 5–7 [13], the oxalate technique suggests precipitation of oxalate complex at lower pH which is more attractive in terms of high yield and simpler realization. According to the calculation of the equilibrium constants and solubility products [14], the optimal pH value at a concentration above 0.02 M for complete deposition of stable barium titanyl oxalate is 4–5 due to the formation of the stable complex Ba^{2+} ions with the oxalate ions under pH above 4, while the complex $TiO(C_2O_4)_2^{2-}$ is formed in the pH range of 1–5 [14]. However, the data regarding the pH region for the high precursor stoichiometry is varied from pH = 2.5 [15] to pH above 3 [14]. When pH is below 1, the mixtures of metal oxalates are deposited, as well as TiO^{2-} ions, which compete with $TiO(C_2O_4)_2^{2-}$ ions. The compound $TiO(OH)_2$ is continued to precipitate at pH above 3 [16], while $TiOH(C_2O_4)$ and $TiOH(OH)_2$ are formed when oxalate ions are in excess. When pH increases above 5, $BaTiO(C_2O_4)_2$ becomes unstable, and the mixture of $TiO(OH)_2$, $Ti(OH)_4$, $TiO(C_2O_4)_2(OH)_2$, TiO_2, $BaCO_3$ as well as jelly-like $BaTiO(OH)_2C_2O_4H_2O$, which requires a higher decomposition temperature, are formed. At such high pH, ions Ba^{2+}

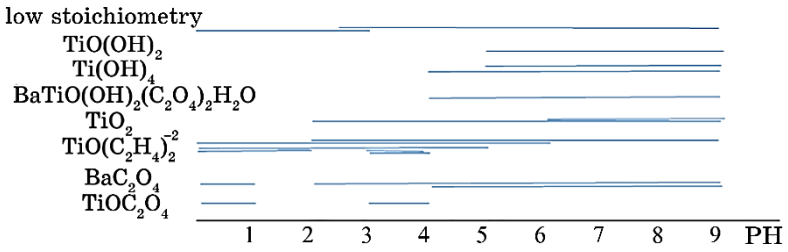

Fig. 1. Illustrative scheme of the phases precipitated at various pH.

are leached, leading to the formation of a Ti-enriched complex [14, 16]. pH diagram exhibit the predominance of the precipitation of the $TiOC_2O_4$, $TiO(C_2O_4)_2^{2-}$ and $TiO(OH)_2$, when pH increase from 1 to 3–4 and above 5, respectively [17]. The $BaTiO_3$ obtained under the modified oxalate method with pH control and O_2 flowing shows that nanopowder obtained at pH 3 instead of 1 results in the precipitation of a mixture of carbonates and oxalates instead of pure oxalate complex, and allows the formation of a single phase of $BaTiO_3$ already at 650–720°C [18]. The typical mechanism of destruction of the precipitated $BaTiO(C_2O_4)_2 \cdot nH_2O$ is described in the line of the papers, where the intermediates are supposed to be presented as $BaTiO(C_2O_4)CO_3$, a mixture of BaO and $TiOC_2O_4$[19], $BaTiO_2(CO)_2$ [20].

Therefore, despite the existed data regarding the possible structure formation at the different pH, the determination/prediction of the complex and its impact on the thermal decomposition behaviour require further studies. To study the impact of the precipitation condition on the thermal decomposition of the precursor and characteristics of the obtained product, the synthesis was carried out in the concentrations range of 0.1–1.5 M and pH of 1–6.

2. MATERIALS AND METHODS

$BaTiO_3$ nanopowder was obtained by the thermal decomposition of the predeposited (Ba, Ti)-based oxalate complex. Titanium tetrachloride ($TiCl_4$), barium chloride ($BaCl_2$), ammonia solution (NH_4OH, 25%), oxalic acid ($H_2C_2O_4$), distilled water (H_2O), and ethanol (C_2H_5OH) were used as starting reagents. To prevent particle growth by the mechanism of Ostwald ripening, precipitation has proceeded under standard conditions. The process was carried out in the concentration range of 0.1–1.5 M and the solution pH of 1–6 under constant stirring. Firstly, a solution of oxalic acid in ethanol was prepared. An aqueous solution of $TiOCl_2$ was added dropwise to a solution of oxalic acid in alcohol with a constant stirring at 200 rpm using a magnetic stirrer 'RCT basic' (IKA), resulting in the formation of the complex $TiO(C_2O_4)_2$. A solution of $BaCl_2$ was added dropwise in order to precipitate the barium titanyl oxalate complex $BaTiO(C_2O_4)_2 \cdot 4H_2O$. To prevent the dissolution of the precipitate at low pH and to support the complete precipitation of the complex $BaTiO(C_2O_4)_2 \cdot 4H_2O$, pH was maintained in the range of 4–6 by a dropwise adding of the solution of ammonia NH_4OH. The final suspension was stirred for 1 h at room temperature and subsequent aging for 20 min for the peptization. The obtained precipitate was decanted using a Buchner funnel, washed with a chlorine solution, and finally washed with ethanol in order to dehydrate the precursor

and to reduce the agglomeration degree. The obtained precipitate was dried at 100°C for 12 h, cooled down in a desiccator, and grounded out in an agate mortar until a homogeneous state.

The determination of the precursor stoichiometry was performed by x-ray fluorescence analysis using x-ray spectrometer Rigaku Primini. Differential thermal analysis of the oxalate precursors was performed at a heating rate of 10°C/min in the air using the Derivatograph (Q-1000). X-ray phase analysis was performed using the diffractometer DRON-3M in CuK_α radiation with a nickel filter. The crystallite size of the precursors was evaluated by Scherrer's formula using data for (101) reflection. The $BaTiO_3$ particle size was evaluated based on the data obtained from the field-emission scanning electron microscopy (FESEM) (Zeiss ULTRA plus).

3. RESULTS AND DISCUSSION

The stoichiometric compound (Ba/Ti = 1.00) was obtained at highest concentration (1.5 M) at lowest pH (1) (Fig. 2, Table 1). The Ba/Ti ratio is increased when pH is increased (at $C = 0.5$ M) while the concentration is decreased (Fig. 2). Therefore, the optimal pH and C for obtaining stoichiometric $BaTiO_3$ are of 4.3 and 1.2 M, respectively.

The deviation from the stoichiometry at low concentration and high pH can be explained by the decrease in the stabilization of Ti^{4+} ions by chlorine ions, while the hydrolysis of Ba and Ti ions is facilitated, leading to the shifting of the equilibrium to the formation of

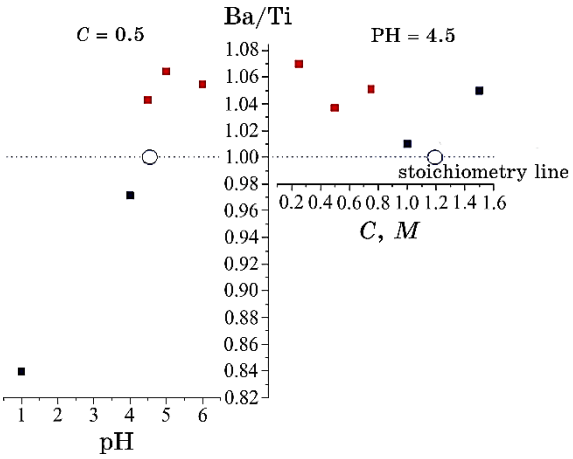

Fig. 2. Dependence of Ba/Ti ratio on the solution pH and reagent concentration. The blue and red colours depict $BaTiO_3$ content above or below 90%, respectively.

TABLE 1. The precipitation condition and characteristics of the obtained products.

pH	C, M	Ba/Ti	T, °C	L, nm	Particle size, nm	Phase
1	0.5	0.83	740	22	28	$BaTiO_3 + TiO_2$am
4	0.5	0.96	720	24	35	$BaTiO_3 + TiO_2$am
1	1.5	1.00	720	34	45	$BaTiO_3$
1	1.5	1.00	720 (n.i.)	22	25	$BaTiO_3$
4.5	1	1.01	770	32	55	$BaTiO_3$
5	0.25	1.03		26	—	$BaTiO_3 + BaCO_3$
4.5	0.5	1.04	967	26	45	$BaTiO_3 + BaCO_3$
4.5	1.5	1.05	890	33	75	$BaTiO_3$
6	0.5	1.05		—	—	$BaTiO_3 + BaCO_3$
4.5	0.75	1.05		25	—	$BaTiO_3 + BaCO_3$
5	0.5	1.06	> 1000	26	—	$BaTiO_3 + BaCO_3$
4.5	0.25	1.07		22	—	$BaTiO_3 + BaCO_3$

the hydroxide of Ti and Ba ions rather than oxalate complex. This leads to the formation of the secondary phase and precursors with composition deviated from $BaTiO(C_2O_4)_2$.

Therefore, at a pH of 4.5, the increase in the reagent concentration from 0.25 M to 1.5 M naturally leads to the shifting in the chemical equilibrium towards the formation of the titanium barium oxalate complex, which, in turn, determines the high stoichiometry of the deposited compounds.

X-ray diffraction analysis of thermally decomposed precursors at a heating rate of 10°C/min showed that the formation of the pure $BaTiO_3$ phase can be achieved in the Ti/Ba ratio range of 0.96–1.01 (Fig. 3), at high concentration and low pH. The deviation from this range leads to the formation of the $BaCO_3$ phase or amorphous TiO_2.

The weight loss curves of the samples 1–1.5, 1–0.5, and 4–0.5 (Fig. 4) with 4 clear regions is consistent with the typical stages of the barium titanyl oxalate decomposition. The TG curves at the whole temperature range, as well as DTA curves at temperatures above 400°C for the mentioned samples are similar indicating the precipitation of the complex with the close structure and the similar decomposition mechanism. Other samples are decomposed at higher temperatures (above 770°C), and the decomposition process includes more than 4 stages, indicating the complexity of the decomposition processes of the system due to the presence of hydro- and carbo-groups.

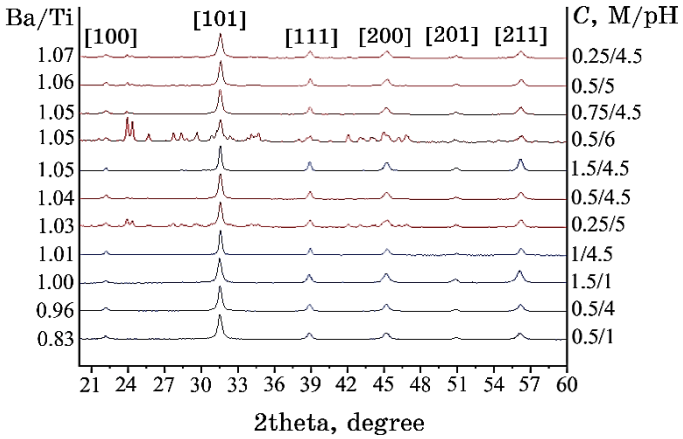

Fig. 3. X-ray diffraction pattern of $BaTiO_3$ nanopowder. The Miller's indexes correspond to the cubic $BaTiO_3$ phase.

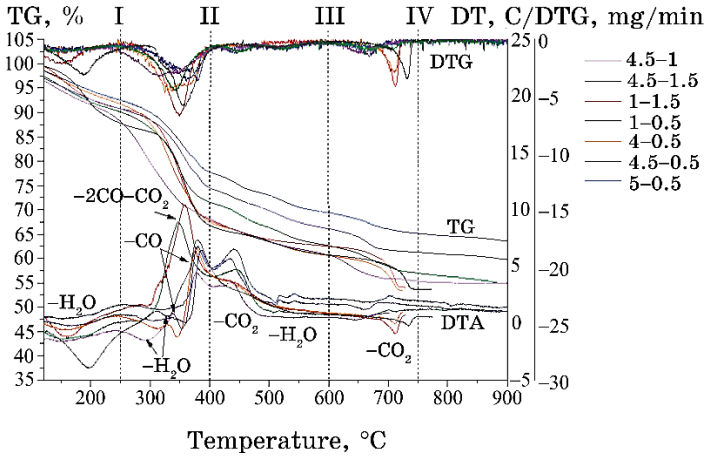

Fig. 4. TG/DT/DTG curves of the samples. Dash lines present the decomposition steps.

At a temperature range of 100–200°C, the dehydration process of the precursor (endothermic peak at 150°C, Fig. 4) is occurred, accompanied by a weight loss of 8–11% (Fig. 3, Table 2). At the next stage (temperature range of 200–400°C), depending on the precipitate composition, the organic complex destruction has occurred with the release of H_2O (endothermic peak at 300–380°C), CO, and CO_2 (exothermic peaks at 330 and 350°C). The weight loss of this process is varied in the range of 13–21%. The weight loss of 5% is well consistent with a value of CO_2 evolved during the gradual de-

TABLE 2. Weight loss during thermogravimetric analysis.

Temperature range, °C	5–0.5	4.5–0.5	4.5–1	4.5–1.5	4–0.5	1–1.5	1–0.5
100–200	9	12	12	12	11	11	13
200–400	13	14	18	16	21	21	20
400–600	9	9	10	11	10	8	7
600–1000	2	3	4	4	4	6	6
	2	2	1	2	—	—	—
Total weight loss, %	36	40	45	45	46	46	46
Water amount	1.9	2.5	2.8	2.8	25	2.5	3.2
Final decomposition temperature, °C	> 1000	970	770	890	720	720	740

composition of $BaTiO(C_2O_4)_2$ through the formation of the intermediate oxycarbonate [21–23]. At the followed step, the exothermic reactions of the crystallization of $Ba_2Ti_2O_5CO_3$ as well as CO_2 desorption from the surface take place, followed by a weight loss of 8–11%.

The final stage is the formation of $BaTiO_3$ starting at a temperature of 600°C due to endothermic reactions of barium carbonate with titanium dioxide as well as decomposition of $Ba_2Ti_2O_5CO_3$ where the weight loss is of 5–6%. Above 720–740°C, no effects or weight loss are observed for samples 1–1.5, 1–0.5, and 4–0.5, indicating the completeness of the crystallization $BaTiO_3$ for the given samples. At the same time, other samples need temperatures higher than 770°C to complete the $BaTiO_3$ crystallization. The total weight loss of each sample in the temperature range of 100–1000°C is 36–46%.

Samples precipitated at the highest *C*, *i.e.*, 1.5 M (1–1.5 and 4.5–1.5) show a strong single exothermic peak at 350°C, referred to the CO and CO_2 liberation ($CO > CO_2$), and the oxidation of CO to CO_2. Together with a high weight-loss value, this may indicate the priority of the decomposition of barium titanyl oxalate through the formation of intermediated oxycarbonates (rather than the oxidation of the precursor to $BaCO_3$ and TiO_2) [22]. The higher exothermic peak of the hydroxo-complex (4.5–1.5, 4.5–1, 4.5–0.5, 5–0.5) appeared at 450°C as compared to the low threshold of the oxalate complex (1–1.5, 1–0.5 and 4–0.5) means the extending of the gas evolution process.

When the concentration is decreased below 1 M (sample 4.5–0.5, 4.5–1), the single peak at 350°C is split into 2 exothermic peaks at 330°C and 380°C while the endothermic peak at 300–380°C has appeared that points to the formation of a hydroxooxalate complex with chemical formulae $BaC_2O_4Ti(OH)_x(C_2O_4)_{2-x/2}$ or $BaC_2O_4TiO_x(OH)_{4-2x}$.

DTG analysis exhibit the release of more oxalate in a sample obtained at pH 4, while more hydroxide in the mixture complexes is obtained at pH = 4.5–5.

When pH is reached value 5 ($C = 0.5$ M), only the endothermic peak at 300–350°C is visible meaning the formation of the hydroxide complex $BaC_2O_4TiO_x(OH)_{4-2x}$. Thus, samples contain different amounts of hydroxide groups in the structure, which, in turn, determines the crystallization mechanism, total weight loss, and amount of water adsorbed at the surface (Table 3).

Thus, the TG, DTG, and DT analysis suggest various structures of the precipitated complex (Table 4) and different schemes of the decomposition for the samples obtained at different synthesis conditions.

When OH content in the structure is increased, the crystallization of the $BaTiO_3$ is started at a lower temperature but more extended in time as compared to the pure oxalate complex leading to the multistep crystallization process caused by the different decomposition temperature and activation energy of the nucleation of the different phases. This, in turn, results in the lower temperature of the $BaTiO_3$ crystallization from the multiphase system, and the formation of smaller crystallite size due to the competition between the nucleation of the different phases and crystal growth inhibition. The crystallite size of $BaTiO_3$ exhibits a direct dependence on the Ba/Ti and the decomposition temperature (Fig. 5).

When the concentration is reduced below 1 M at pH 4.5, the complex structure has deviated from the stoichiometry (Ba/Ti above 1) leading to the formation of $BaCO_3$ as a secondary phase. In this case, the crystallite size is determined predominantly by the competition between the nucleation and growth in the multiphase system rather than the decomposition temperature. Particularly, the formed $BaCO_3$ inhibits the $BaTiO_3$ growth and the mean crystallite size of $BaTiO_3$ is 26 nm.

Similarly, to the crystallite size, the increase in pH or C in the deposition process leads to an increase in the $BaTiO_3$ particle size (Fig. 6). Thus, in the pH line 1–4–4.5 at $C = 0.5$ M, the particle size is 28–35–45 nm.

When C increase in the line 0.5–1–1.5 M at pH = 4.5, the particle size is of 45–55–75 nm.

The smallest particle size (of 28 nm) and narrowest particle size distribution (Fig. 7) are observed for the sample obtained at the lowest pH (1) and C (0.5 M). However, if the stoichiometric $BaTiO_3$ 1–1.5 is decomposed *via* non-isothermal mode [24], the size of the crystallite and particle (sample 1–1.5 n.i.) reach a similar to non-stoichiometric compound value, particularly 22 nm and 25 nm, respectively (Table 1, Fig. 6).

TABLE 3. Decomposition mechanism for the different structure.

Structure name	Possible mechanism	Theoretical total weight loss at different water amount, %			
		1	2	3	4
A	$BaTiO(C_2O_4)_2nH_2O \rightarrow BaTiO_3 + nH_2O + 2CO + 2CO_2$	41.00	43.57	45.93	48.10
B	$BaTi(OH)_2(C_2O_4)_2nH_2O \rightarrow BaTiO_3 + (n+1)H_2O + 2CO + 2CO_2$	43.57	45.93	48.10	50.10
C	$BaTiO(OH)_2C_2O_4nH_2O \rightarrow BaTiO_3 + (n+1)H_2O + CO + CO_2$	31.66	35.09	38.19	41.01
D	$BaC_2O_4Ti(OH)_4nH_2O \rightarrow BaTiO_3 + (n+2)H_2O + CO + CO_2$	35.09	38.19	41.01	43.58

TABLE 4. Structure of the samples.

Sample	Structure name	Structure	Crystallite size, nm	Particle size, nm
1–0.5/1–1.5	A	$BaTiO(C_2O_4)_2nH_2O$	22/29	28/45
4–0.5	B	$BaTiO_x(OH)_{2-2x}(C_2O_4)_2nH_2O$ ($x = 0$–1)	24	35
4.5–0.5	C	$BaTiO_x(OH)_{4-2x}C_2O_4nH_2O$ ($x = 0$–1)	26	45
4.5–1/4.5–1.5	D	$BaTi(OH)_x(C_2O_4)_{3-x/2}nH_2O$ ($x = 2$–4)	32/33	55/75

Thus, the smallest crystallite and particle size of the $BaTiO_3$ is obtained from the oxalate complex (Fig. 8) due to the facilitation of the product crystallization with high Cl-ion concentration, additional nucleation centres from the TiO_2 amorphous phase at the lowest pH (1), as well as due to the minor particle collisions at lowest C (0.5 M).

The average size of $BaTiO_3$ crystallite and particle were almost

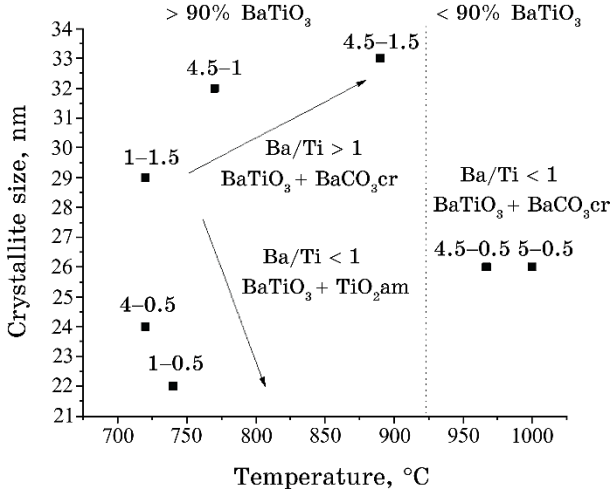

Fig. 5. The variations of the crystallite size with the temperature.

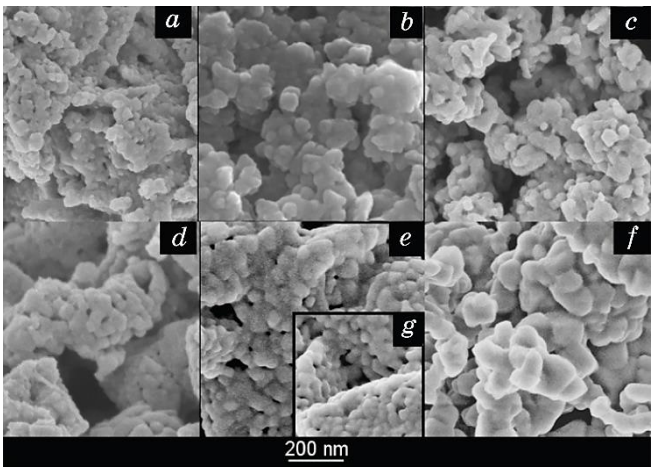

Fig. 6. SEM images of $BaTiO_3$ obtained from the precursor deposited at different condition. *a*—4–0.5; *b*—1–0.5; *c*—4.5–0.5; *d*—4.5–1; *e*—1–1.5; *f*—4.5–1.5; *g*—1–1.5.

the same at low C and pH, while, at the high values, a large difference between them is observed, meaning the formation of several crystallites in an individual particle or the formation of an amorphous secondary phase at surface of $BaTiO_3$.

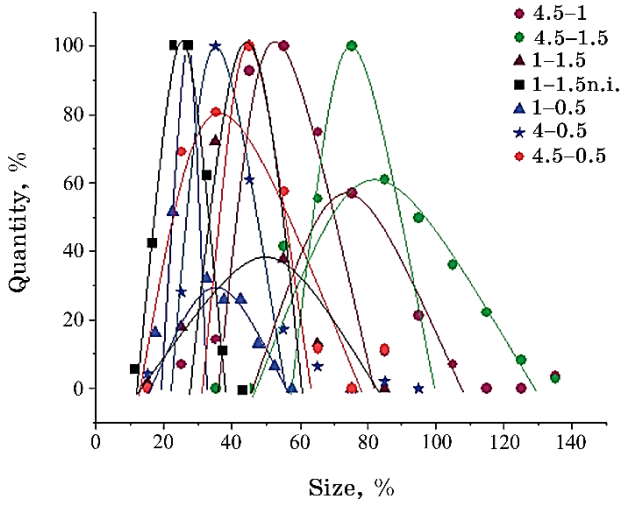

Fig. 7. Size distribution of the $BaTiO_3$ nanoparticles obtained from the precursors deposited at different condition.

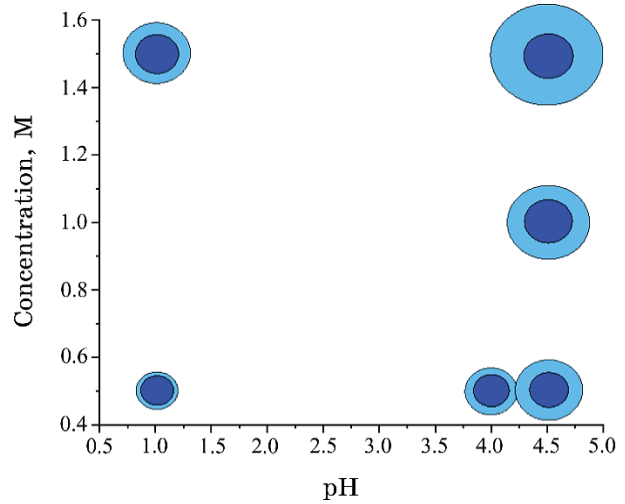

Fig. 8. The effect of the synthesis condition on the crystallite size of the $BaTiO_3$ (blue) and particle size (sky-blue).

4. CONCLUSIONS

The oxalate method allows obtaining stoichiometric nanoparticles with the desired size, which is important for controlling the properties of the final material based on such nanoparticles. It was shown that the stoichiometric $BaTiO_3$ (Ba/Ti = 1) may be obtained at C of 1.5 M and pH of 1. The formation of the multiphase system, especially, if Ba/Ti < 1, induces the formation of smaller crystallite size as compared to the pure phase. The decomposition temperature of the samples with Ba/Ti < 1 is of 720–740°C, while the hydroxide and carbonate samples with Ba/Ti > 1 are decomposed at a temperature of above 770°C. At the highest C (1.5 M), the decomposition of barium titanyl oxalate goes through the formation of intermediated oxycarbonates rather than the oxidation of the precursor to $BaCO_3$ and TiO_2. The calcination of the stoichiometric $BaTiO_3$ via non-isothermal mode leads to the formation of $BaTiO_3$ with crystallite and particle sizes of 22 nm and 25 nm, respectively.

ACKNOWLEDGMENTS

We are grateful to Srečo Davor Škapin from Jožef Stefan Institute for the SEM analysis.

REFERENCES

1. S. B. Basturk, C. E. J. Dancer, and T. McNally, *J. Appl. Polym. Sci.*, **138**, No. 22: 50521 (2021); https://doi.org/10.1002/app.50521
2. J. Chen, X. Liu, Z. Shen, and G. Chu, *High-Gravity Reactive Precipitation Process for the Preparation of Barium Titanate Powders*: Patent US 8715614, US10/624,944 (2014).
3. P. Kumar, S. Singh, M. Spah, J. K. Juneja, C. Prakash, and K.K. Raina, *J. Alloys Compd.*, **489**: 59 (2010); https://doi.org/10.1016/j.jallcom.2009.08.024
4. G. Panomsuwan and H. Manuspiya, *Mater. Res. Express*, **6**, No. 6: 065062 (2019); https://doi.org/10.1088/2053-1591/ab101b
5. A. Shi, *J. Cent. South Univ. Technol.*, **15**, No. 3: 334 (2008); https://doi.org/10.1007/s11771-008-0063-2
6. K. M. Hung, W. D. Yang, and C. C. Huang, *J. Eur. Ceram. Soc.*, **23**: 1901 (2003); https://doi.org/10.1016/S0955-2219(02)00431-4
7. H. Xu and L. Gao, *Mater. Lett.*, **57**, No. 2: 490 (2002); https://doi.org/10.1016/S0167-577X(02)00817-0
8. L. Guo, H. Luo, J. Gao, L. Guo, and J. Yang, *J. Mater. Lett.*, **60**, No. 24: 3011 (2006); https://doi.org/10.1016/j.matlet.2006.02.035
9. W. S. Clabaugh, E. M. Swiggard, and R. Gilchrist, *J. Res. Natl. Bur. Stand.*, **56**, No. 5: 1 (1956).
10. R. A. Kimel, V. Ganine, and J. H. Adair, *J. Am. Ceram. Soc.*, **84**: 1172

(2001); https://doi.org/10.1111/j.1151-2916.2001.tb00809.x
11. S. Wada, T. Hoshina, H. Yasuno, S. M. Nam, H. Kakemoto, and T. Tsurumi, *Key Eng. Mater.*, **248**: 19 (2003); https://doi.org/10.4028/www.scientific.net/KEM.248.19
12. C. J. Huang, K. L. Chen, P. H. Chiu, P. W. Sze, and Y. H. Wang, *J. Nanomater.*, Article ID 718918 (2014); https://doi.org/10.1155/2014/718918
13. G. K. Sahoo, *Synthesis and Characterization of Zr and Ca Modified $BaTiO_3$ Ferroelectric Ceramics* (Doctoral dissertation) (2015).
14. 노태용;김승원;이철; *Bull. Korean Chem. Soc.*, **16**: 1180 (1995); https://doi.org/10.5012/bkcs.1995.16.12.1180
15. A. V. Prasadarao, M. Suresh, and S. Komarneni, *Mater. Lett.*, **39**, No. 6: 359 (1999); https://doi.org/10.1016/S0167-577X(99)00035-X
16. C. Szepesi, *Synthesis and Processing of Submicron Barium Titanyl Oxalate Tetrahydrate* (Doctoral dissertation) (Penn. State Univ.: 2004).
17. F. Schrey, *J. Am. Ceram. Soc.*, **48**, No. 8: 401 (1965); https://doi.org/10.1111/j.1151-2916.1965.tb14776.x
18. J. E. Jeon, H. S. Han, K. R. Park, Y. R. Hong, K. Bo Shim, and S. Mhin, *Ceram. Int.*, **44**: 1420 (2018); https://doi.org/10.1016/j.ceramint.2017.09.231
19. V. M. Pogibko, V. V. Prisedskiy, and I. L. Sidak, *Voprosy Khimii i Khimicheskoi Tekhnologii* [Issues of Chemistry and Chemical Technology], p. 96 (2010).
20. P. K. Gallagher and J. Thomson, *J. Am. Ceram. Soc.*, **48**: 644 (1965); https://doi.org/10.1111/j.1151-2916.1965.tb14697.x
21. O. O. Vasyl'kiv, A. V. Ragulya, and V. V. Skorokhod, *Powder Metall. Met. Ceram.*, **36**, No. 5: 277 (1997); https://doi.org/10.1007/BF02676217
22. O. O. Vasyl'kiv, A. V. Ragulya, V. P. Klimenko, and V. V. Skorokhod, *Powder Metall. Met. Ceram.*, **36**, No. 11: 575 (1997); https://doi.org/10.1007/BF02676141
23. W. S. Jung, B. K. Min, J. Park, and D. H. Yoon, *Ceram. Int.*, **37**: 669 (2011); https://doi.org/10.1016/j.ceramint.2010.09.056
24. A. V. Ragulya, O. O. Vasyl'kiv, and V. V. Skorokhod, *Powder Metall. Met. Ceram.*, **36**, No. 3: 170 (1997); https://doi.org/10.1007/BF02676084